Abnormal Cross Frequency Coupling of Brain Electroencephalographic Oscillations Related to Visual Oddball Task in Parkinson's Disease with Mild Cognitive Impairment

Clinical EEG and Neuroscience
1–12

DOI: 10.1177/15500594221128713
journals.sagepub.com/home/eeg
SAGE

Abnormal Cross Frequency Coupling of Brain Electroencephalographic Oscillations Related to Visual Oddball Task in Parkinson's Disease with Mild Cognitive Impairment

Zübeyir Bayraktaroğlu[1,2], Tuba Aktürk[3,4,5], Görsev Yener[6,7], Tom A. de Graaf[5], Lütfü Hanoğlu[2,4,8], Ebru Yıldırım[3,4], Duygu Hünerli Gündüz[9], İlayda Kıyı[9], Alexander T. Sack[5], Claudio Babiloni[10,11], and Bahar Güntekin[4,12]

Abstract

Parkinson's disease (PD) is a movement disorder caused by degeneration in dopaminergic neurons. During the disease course, most of PD patients develop mild cognitive impairment (PDMCI) and dementia, especially affecting frontal executive functions. In this study, we tested the hypothesis that PDMCI patients may be characterized by abnormal neurophysiological oscillatory mechanisms coupling frontal and posterior cortical areas during cognitive information processing. To test this hypothesis, event-related EEG oscillations (EROs) during counting visual target (rare) stimuli in an oddball task were recorded in healthy controls (HC; N = 51), cognitively unimpaired PD patients (N = 48), and PDMCI patients (N = 53). Hilbert transform served to estimate instantaneous phase and amplitude of EROs from delta to gamma frequency bands, while modulation index computed ERO phase-amplitude coupling (PAC) at electrode pairs. As compared to the HC and PD groups, the PDMCI group was characterized by (1) more posterior topography of the delta-theta PAC and (2) reversed delta-low frequency alpha PAC direction, ie, posterior-to-anterior rather than anterior-to-posterior. These results suggest that during cognitive demands, PDMCI patients are characterized by abnormal neurophysiological oscillatory mechanisms mainly led by delta frequencies underpinning functional connectivity from frontal to parietal cortical areas.

Keywords

parkinson's disease, parkinson's disease with mild cognitive impairment (PDMCI), brain event-related oscillations (EROs), cross-frequency coupling, phase-amplitude coupling, oddball paradigm

Received January 28, 2022; revised July 11, 2022; accepted September 6, 2022.

[1]International School of Medicine, Department of Physiology, Istanbul Medipol University, Istanbul, Turkey
[2]Research Institute for Health Sciences and Technologies (SABITA), functional Imaging and Cognitive Affective Neuroscience Research Laboratory (fINCAN), Istanbul Medipol University, Istanbul, Turkey
[3]Vocational School, Program of Electroneurophysiology, Istanbul Medipol University, Istanbul, Turkey
[4]Research Institute for Health Sciences and Technologies (SABITA), Clinical Electrophysiology, Neuroimaging and Neuromodulation Laboratory, Istanbul Medipol University, Istanbul, Turkey
[5]Faculty of Psychology and Neuroscience, Department of Cognitive Neuroscience, Section Brain Stimulation and Cognition, Maastricht University, Maastricht, Netherlands
[6]Dokuz Eylul University Health Campus, Izmir Biomedicine and Genome Center, Izmir, Turkey
[7]Faculty of Medicine, Izmir University of Economics, Izmir, Turkey
[8]School of Medicine, Department of Neurology, Istanbul Medipol University, Istanbul, Turkey
[9]Institute of Health Sciences, Department of Neurosciences, Dokuz Eylül University, Izmir, Turkey
[10]Department of Physiology and Pharmacology "V. Erspamer", Sapienza University of Rome, Rome, Italy
[11]Hospital San Raffaele of Cassino, Cassino, Italy
[12]School of Medicine, Department of Biophysics, Istanbul Medipol University, Istanbul, Turkey

Corresponding Author:
Bahar Güntekin, Department of Biophysics, School of Medicine, Istanbul Medipol University, Istanbul, Turkey.
Email: bguntekin@medipol.edu.tr

Introduction

Parkinson's disease (PD) is a movement disorder, mainly caused by degeneration in dopaminergic neurons of substantia nigra affecting basal ganglia circuits and cognitive motor functions. Notably, those circuits modulate several cognitive functions including frontal executive functions (ie, attention and working memory, decision-making, etc), learning, and episodic memory.[1] During the disease course, those dysfunctions in these circuits are associated to a clinical syndrome progressing from mild cognitive impairment (MCI) to dementia in most PD patients.[2–6]

In the framework of a Precision Medicine approach, PD patients should be periodically assessed according to their (1) cognitive status by neuropsychological "paper and pencil" tests and (2) brain neurophysiological functioning by adequate biomarkers. Informative biomarkers of brain neurophysiological functioning may derive from the analysis of electroencephalographic (EEG) oscillatory activity recorded during cognitive demands. This activity reflects event-related oscillations (EROs) in cortical neural excitability during sensory information processing and can provide useful information on the derangement of brain cognitive systems in patients with PD or other neurodegenerative disorders.[7,8]

In previous studies, topographically widespread EROs during auditory and visual cognitive tasks were lower in magnitude at delta (<4 Hz) and theta (4-7 Hz) frequencies in PDMCI patients when compared to PD patients without cognitive deficits and healthy cognitively unimpaired control (HC) persons.[9–14] Notably, similar abnormalities in EROs were found in patients with cognitive deficits due to Alzheimer's disease, so these biomarkers may be not specific for PD effects on brain cognitive systems.[15] Nevertheless, EROs may be useful to appreciate the extent to which brain cognitive systems at work are disrupted in PD patients with the same medical diagnosis.

A new frontier in the study of EROs during cognitive tasks is the computation of the statistical interdependence (coupling) of those oscillations at different frequency bands and scalp electrodes, as a reflection of multi-scale integration of neural activity in cortical cognitive networks at work.[16] This statistical interdependence is generally referred to as cross-frequency coupling (CFC) of resting state EEG activity or EROs during cognitive tasks at a given scalp electrode (cortical source) or scalp electrode (cortical source) pair. Notably, CFCs from those EEG signals can be observed at different scales in the brain, from invasive intracerebral to scalp-recorded EEG or ERO signals.[7,17–20] While the statistical interdependence (coupling) between high-frequency EEG oscillations (>30 Hz within beta and gamma frequency bands) at an electrode pair is usually significant only in close proximity to their cortical EEG sources, that between EROs slower on frequency (<8 Hz within delta and theta frequency bands) is significant for more widespread ranges in the cortical source space.[21] This typical observation suggests that EROs at delta and theta frequencies may integrate cognitive information processing over larger spatial scales, while EROs at beta and gamma frequencies may play a role in local cognitive information processing.[21,22]

Several variants of CFC of EEG or ERO activity have been defined, such as frequency-frequency amplitude-amplitude coupling, and phase-amplitude-coupling (PAC), both at a given scalp electrode (cortical source) or electrode pair.[23] Among them, the CFC based on PAC quantifies the modulation of the EEG or ERO amplitude at a given frequency and electrode (source) by the phase of another frequency band. The same concept has been applied to the CFC based on PAC computed at a given frequency and electrode pair.[23]

In physiological conditions,[24–26] the phase of EEG oscillations at theta frequencies (~6 Hz) in the hippocampus was shown to modulate the amplitude of local gamma EEG oscillations (~40 Hz) as a neurophysiological underpinning of the ability to hold a (limited) number of items available for cognitive processing, namely the short-term memory capacity. Several studies extended these CFC based on PAC findings on the electrophysiological data recorded at multiple spatial scales in several brain regions for investigating other cognitive functions such as attention,[27] decision making,[27,28] and sensory detection.[29] In parallel to this prominent theta-gamma PAC, a large number of EEG studies reported other CFC based on PACs (in the related-brain regions), such as delta-beta coupling as an indicator of cortical-subcortical control of motivational and emotional processes,[30] temporal prediction, and prediction accuracy,[31] and social anxiety.[32]

In pathophysiological conditions, abnormal CFC from EEG activity was associated with cognitive impairment.[33] Specifically, it happened in patients with schizophrenia,[34] epilepsy,[35] and Alzheimer's disease.[36,37] Furthermore, power-to-power and phase-to-amplitude CFCs from EEG activity were also abnormal in PD patients in relation to motor symptoms.[19,20] Notably, no previous study investigated the CFC based on PAC from cognitive EROs in PD patients with cognitive deficits, typically involving frontal executive functions.

The importance of anterior-posterior connectivity in cognition (and impairment in some pathologies) is the point on which the study's central hypothesis is based.[38–41] Therefore, in this study, we tested the hypothesis that PDMCI patients may be characterized by abnormal neurophysiological oscillatory mechanisms coupling specifically between frontal and posterior cortical areas during cognitive information processing as revealed by the CFC based on cognitive EROs. To test this hypothesis, EROs during counting visual target (rare) stimuli in a standard oddball task intermingling those stimuli with frequent ones were recorded in healthy controls (HC), cognitively unimpaired PD patients, and PDMCI patients. Furthermore, that CFC from EROs at electrode pairs was used as a measure of underlying cortical functional connectivity between frontal and posterior areas during cognitive information processing.

Method

Participants

The participants were recruited into three study groups: PD (N = 48) only with motor symptoms, PDMCI (N = 53), and healthy controls (HC, N = 51). The demographics of the participants are given in Table 1. All participants had normal or corrected-to-normal vision.

The patients with PD were diagnosed by the neurology specialists according to the "United Kingdom Parkinson's Disease Society Brain Bank" criteria.[42] Litvan's criteria were used for the diagnosis of PDMCI.[43] The participants were assessed extensively with neuropsychological tests in several cognitive domains including memory processes, language abilities, executive functions, attention, and visuospatial skills (see supplementary for details). Additionally, the Turkish version of the standardized Mini-Mental State Examination (MMSE).[44,45] was employed to assess the general cognitive states. The dementia stage was determined by the Clinical Dementia Rating scale (CDR).[46] The Unified Parkinson's Disease Rating Scale (UPDRS)[47] was applied to evaluate the severity of PD. UPDRS scores of the patient groups were given in Table 1. To establish the stage of the disease, the Hoehn-Yahr scale[48] was used. All participants in PD and PDMCI groups were on stage 3 or below.

The history of severe head trauma, drug abuse or chronic alcoholism, and any other neurological or psychiatric disease (eg, mood disorders and schizophrenia) or Parkinson plus syndromes were exclusion criteria for the PD and the PDMCI group. In addition to these, any cognitive impairment according to the neuropsychological assessments were exclusion criteria for the HC group. All patients with PD were included in the assessments after taking their daily levodopa (equivalent) dose.

The study was approved by the local ethics committee (no. 10840098-51). Oral and written informed consents was obtained from all participants and/or their caregivers who approved their participation in the study.

Experimental Design

The visual oddball paradigm was the cognitive task during the EEG recordings. A total of 120 stimuli that consisted of 40 targets and 80 non-targets were presented. Before the experiment began, a short version of the paradigm was presented for practice. Two different diffuse screen luminance levels were defined as target (10 cd/cm^2) and non-target (40 cd/cm^2) stimuli. The participants were asked to mentally count the number of target stimuli while ignoring the non-targets. At the end of the experiment, they were asked for the total number of target stimuli to assess their task performance. Based on these self-reported behavioral outputs, oddball task scores of the participants were calculated. In the calculations of the scores, deviated numbers from the correct target number (40 targets) were considered as participants' error scores.

The stimulus duration was 1000 ms and the interstimulus interval was randomly varied between 3 to 7 s. The stimuli were displayed on a 19" square screen (refresh rate 60 Hz) which was located 120 cm away from the participants.

EEG Recordings

EEG was recorded from 30 Ag/AgCl scalp electrodes with EasyCap (EasyCap GmbH, Germany) according to the

Table 1. Demographic Data and MMSE, Stroop, Oddball Error and UPDRS (Motor) Scores.

	HC (N = 51) M ± SD	PD (N = 48) M ± SD	PDMCI (N = 53) M ± SD	*P*
Age	66.7 ± 9.9	65.3 ± 7.7	66.9 ± 8.4	.124[a]
Education	10.1 ± 4.9	9.5 ± 4.7	7.9 ± 4.8	.065[a]
Gender	♀ 28 ♂ 23	♀ 15 ♂ 33	♀ 12 ♂ 41	**.002**[b]
MMSE	28.3 ± 1.7	27.8 ± 2.0	24.6 ± 4.6	0.200 (HC vs PD)[c] **<0.05 (HC vs PDMCI)**[c] **< 0.05 (PD vs PDMCI)**[c]
Stroop	51.9 ± 16.5	52.2 ± 17.6	82.7 ± 25.5	0.935 (HC vs PD)[c] **<0.001 (HC vs PDMCI)**[c] **< 0.001 (PD vs PDMCI)**[c]
Oddball error score	0.51 ± 0.88	2.29 ± 2.74	4.17 ± 5.31	**<0.001 (HC vs PD)**[c] **<0.001 (HC vs PDMCI)**[c] **< 0.05 (PD vs PDMCI)**[c]
UPDRS	—	19.7 ± 7.6	20.6 ± 8.5	.425[c]
Disease Duration	—	4.0 ± 3.5	4.5 ± 4.0	.570[c]

♀: Female; ♂: Male.

Abbreviations: M, Mean; SD, standard deviation; HC, healthy controls; PD, Parkinson's disease; PDMCI, Parkinson's disease with mild cognitive impairment; MMSE, mini-mental state examination test; UPDRS, unified Parkinson's disease rating scale.

[a]One-way ANOVA.

[b]Chi-square test.

[c]Two-sample *t*-test.

extended 10-20 electrode placement system. Two physically linked electrodes placed on the right and the left earlobes served as references. The ground electrode was placed behind the right earlobe. The electrooculogram was recorded from the electrodes on the nasion and outer canthus of the right eye and referenced to each other. BrainAmp DC amplifier (Brain Product GmbH, Germany) was used for EEG recordings with 0.01-250 Hz analog input filter and the sampling rate of 500 samples/s. Impedances for all recording electrodes were kept below 10 KOhm, and below 5 KOhm for the reference and ground electrodes. The participants were seated in a dimly lit, soundproof, and electromagnetically shielded room for EEG recordings.

EEG Analysis

All EEG preprocessing and statistical analysis steps were performed in MATLAB (ver. 2019b) environment using the BBCI Toolbox[49] developed in MATLAB along with the MATLAB core functions and Statistical Analysis Toolbox (Mathworks Inc, USA). The head-in-head plots produced with the showcs.m function from the METH toolbox by Guido Nolte.[50]

EEG Preprocessing. Continuous EEG signals bandpass filtered between 0.01 and 45 Hz with Butterworth second order filter with zero phase distortion only to mark the segments with artifacts. The filtered EEG signals were split into epochs spanning the time 500 ms before and 1000 ms after the stimulus for modulating delta frequency, for higher modulating frequencies epoch limits were 500 ms before and 500 ms after stimulus. The epochs were baseline corrected for the mean EEG amplitude of 200 ms before each stimulus. Artifact rejection was done semi-automatically on the epoched EEG data. The automatic rejection criteria were 150 μV amplitude differences between the minimum and the maximum samples or absolute amplitude larger than 80 μV in the epoch of interest, and differences larger than 50 μV between two consecutive samples in an epoch. The amplitudes lower than 0.1 μV for more than 20 ms were marked as low activity. Additionally, automatically marked artifacts and the epochs with low EEG amplitude were inspected visually by an expert, and muscle, eye or movement artifacts not detected by the algorithm were also marked. The epochs with artifacts marked on the raw EEG data were removed from further analysis.

Calculation of Cross-Frequency Coupling Based on Phase Amplitude Coupling. The CFC based on PAC was computed from the artifact-free EROs associated with the visual rare (target) stimuli. Specifically, it was calculated between the phase of a lower frequency and the amplitude of a higher frequency signal in target epochs between electrode pairs. The CFC based on PAC analysis was constrained to 18 electrodes representative of frontal, central, parietal, and occipital scalp regions of interest (F3, Fz, F4, FC3, FCz, FC4, C3, Cz, C4, CP3, CPz, CP4, P3, Pz, P4, O1, Oz, O2). The remaining electrodes, mostly located in the border of the scalp were more prone to residual muscular and ocular artifacts and would have possibly inflated computational solutions and statistical comparisons.

The CFC based on PAC was calculated between canonical EEG frequency bands strictly following the procedure described in the reference study by Tort et al (2010).[51] The EEG frequency bands were defined as follows: delta (0.5-3.5 Hz), theta (4-7 Hz), low-frequency alpha (7-11 Hz), high-frequency alpha (9-13 Hz), beta (15-25 Hz), and gamma (35-45 Hz).

The continuous raw EEG data of the EROs were band-pass filtered in the modulating (delta, theta) and modulated (theta, low-frequency alpha, high-frequency alpha, beta, gamma) frequency bands. Specifically, the EROs were filtered around a center frequency at the described frequency bands with a fourth order, zero phase-shift Butterworth filter. The bandwidth for the delta and theta bands were ± 1 Hz, for alpha was ± 2 Hz, and for the beta and gamma bands were ± 5 Hz. Instantaneous phase and amplitude values were calculated on the filtered EROs between electrode pairs by the Hilbert transform using the hilbert.m function in MATLAB. The CFC based on PAC was calculated on the segmented data for 1000 ms and 500 ms time periods after the rare (target) stimulus presentation for the delta and theta modulating-frequencies, respectively. The amplitude of the modulated EEG signals was binned as a function of the phase of the modulating frequencies, and the normalized mean amplitude was calculated for bins by dividing each bin value by the sum over the bins at a single electrode level. Modulation index (MI) was calculated as a measure of the amount of PAC between EROs at a given electrode pair with 15-degree phase angle resolution.[51] The modulating (phase) and modulated (amplitude) frequency pairs over the CFC calculated are reported in Table 2. Mean CFC values for each group are visualized as head-in-head plots as introduced by Nolte et al (2014)[50] for each frequency pair of CFC values (Supplementary Figures 1 to 3).

Substantial CFC Testing. In the present study, we followed the common practice to compare the MI values computed from EROs for a given electrode pair and subject against the distribution of MI values computed from surrogate EEG time series mathematically generated to have statistical properties (eg, EEG power density, signal-to-noise ratio, etc) similar to EROs.[51–54] For this purpose, the amplitude of the modulated higher-frequency EEG segments was randomly shuffled

Table 2. The Modulating (Phase) and Modulated (Amplitude) Frequency Pairs for MI Were Calculated.

CFC Pairs		Modulated				
		theta	low alpha	high alpha	beta	gamma
Modulating	delta	x	x	x	x	x
	theta	—	x	x	x	x

concerning the phase of the modulating lower-frequency EEG segments. As a result, we generated 1000 surrogate MI values for each electrode and frequency pair (Table 2) to establish the MI distribution computed at the chance level (alpha = 0.05). Afterward, we defined significance thresholds individually as a MI value greater than 1.96 SD from the mean value. Furthermore, we transformed all measured MI values to z values by subtracting the mean and dividing them into the SD of the null distribution for each subject for given frequency pairs. For practicality as in the common practice, we considered z transformed MI values $z \geq 2$ significant (determined according to the standard normal distribution), which approximately corresponds to $p < .05$, namely 95% confidence level. In the procedure explained here, within-subject values were tested to assess substantial CFC values at the individual level compared to the CFC values from surrogated data. This procedure was used to determine the data which had the robust CFC to be used in between-subject statistical analysis (in ANOVAs).

The CFC based on PAC from EROs was calculated for all combinations of 18 electrodes and each frequency band, so producing 324 MI values for each subject. The topographical distribution of the mean MI values (z transformed) for all subjects and 3 groups (HC, PD, and PDMCI) is shown in Supplementary Figure 1 for 3 different CFCs based on PAC electrode pairs. Figures 1 to 3 show a matrix-wise representation of these values across all subjects and 3 groups.

Statistical Analysis

EEG. The electrode pairs of interest for the statistical analysis were selected with the guidance of the topographical distribution of the mean CFC based on PAC values in the head-in-head plots (Supplementary Figure 1) and the CFC matrices (Figures 1 to 3) for groups.

Figures 1 to 3 illustrated the changes of the CFC based on PAC from EROs among the fronto-central and parieto-occipital sites for each group of persons. For data reduction purposes, we pooled electrodes in the following scalp regions of interest: fronto-central (F3, Fz, F4, FC3, FCz, FC4) and parieto-occipital (P3, Pz, P4, O1, Oz, O2), which were denoted as FC (anterior) and PO (posterior), respectively. Afterward, we calculated mean z values for each subject and electrode and moved to the statistical comparisons between the groups.

Due to head volume conduction effects, a certain amount of CFC based on PAC from EROs can be observed between all electrode pairs. Therefore, we create a null distribution to define a threshold to eliminate "fake" CFCs from EROs as mentioned above ($z \geq 2$).

The robustness of the CFC based on PAC values was controlled using the number of z values under 2 for each electrode pair per subject for a given frequency pair. If the number of CFC pairs (n = 324) with low values was 3 SD away from the population mean, these subjects were removed from further evaluation of the frequency pair (delta-theta: 3 subjects (1 subject from each group); delta-low alpha: 4 subjects (1 from HC, 1 from PD, 2 from PDMCI); delta-high alpha: 1 subject from PDMCI group).

The mean z values pooled from the fronto-central (anterior) and parieto-occipital (posterior) electrodes formed 4 modulating and modulated electrodes for each frequency pair: Anterior-to-Anterior (AA), Anterior-to-Posterior (AP), Posterior-to-Anterior (PA), and Posterior-to-Posterior (PP). These four modulating and modulated electrode pairs were used in ANOVA design as the level of location within-subject factor.

The repeated measures ANOVA test with the 3-by-4 mixed design was performed for each CFC based on the PAC frequency pair where the 3 groups were defined as the between-subjects factor (Group: HC, PD, PDMCI) and 4 modulating-modulated electrode pairs (Location: AA, AP, PA, PP) as within-subject factors.

The raw MI values distributed exponentially, therefore, to make data more amenable for the F-test we used the z values for statistical analysis. Because the sphericity condition was not met as controlled with the Mauchly method,[55] we reported the Greenhouse-Geisser corrected p values in the results section.

Results

Behavioral

MMSE was used to assess general cognitive functioning while the Stroop test more specifically targeted the frontal-executive functions. Therefore, these tests' scores and additionally visual oddball task performance were compared across the groups. Results showed that MMSE and Stroop scores were decreased in the PDMCI group compared to both PD and HC groups (ps<0.05) while there was no difference between PD and HC (ps>0.05) (Table 1). For the oddball task scores, PDMCI had lower scores than the PD and HC groups (ps<0.05), and HC group had better scores than both PD and PDMCI groups (ps<0.05) (Table 1).

Additionally, these task/test scores were used in the correlation analyses as cognitive measures (see supplementary).

EEG

Three out of 9 CFC based on PAC electrode pairs, as defined in Table 2, were statistically tested for between-group differences, namely, delta-theta, delta-low frequency alpha, and delta-beta coupling. The other CFC pairs were eliminated from further analysis because not enough subjects remained in the study groups with robust CFC, when the electrode pairs and the subjects with CFC under the threshold (z < 2) were removed. In the following sections, we reported statistical results for delta-theta, delta-low frequency alpha, and delta-beta coupling, which showed statistically significant effects in the comparison among the groups ($p < .05$).

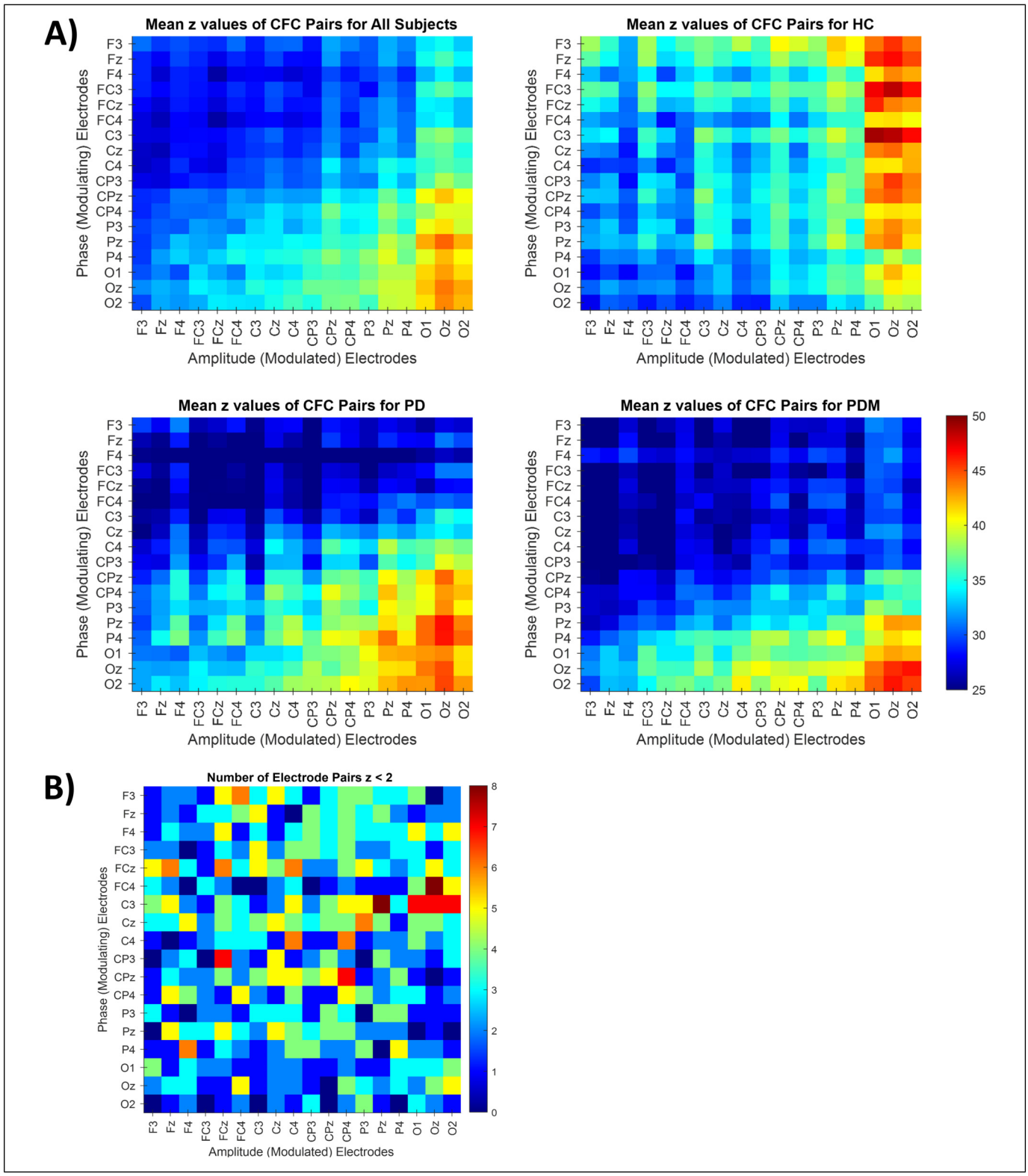

Figure 1. (A) Z values for delta-theta CFC between all electrode pairs. The mean z values for all subjects, healthy controls, Parkinson's Disease, Parkinson's Disease with MCI. HC: Healthy Controls; PD: Parkinson's Disease; PDM: PD with MCI. (B) The number of subjects where $z < 2$ in a specific electrode pair.

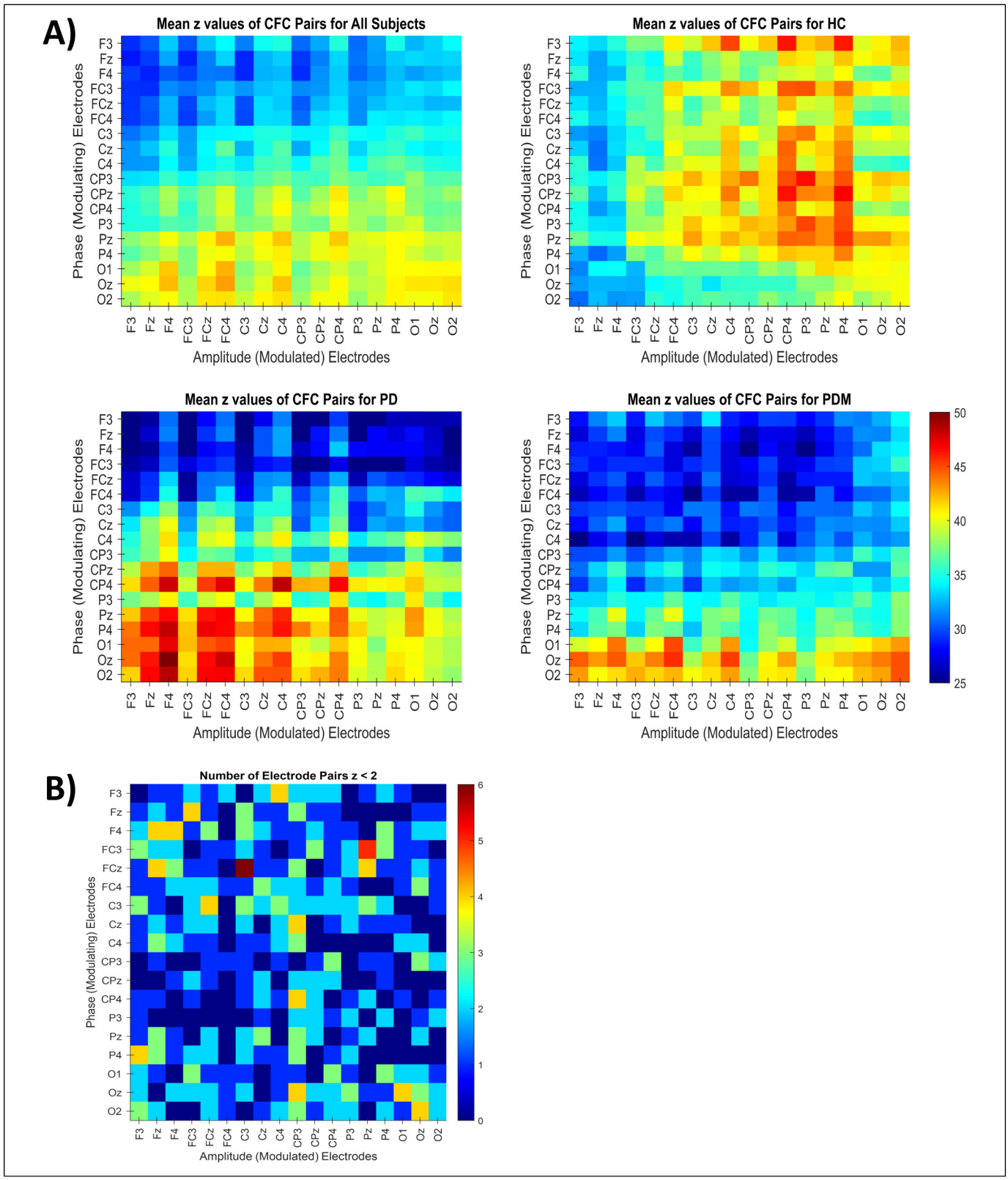

Figure 2. (A) Z values for delta-low frequency alpha CFC between all electrode pairs. The mean z values for all subjects, healthy controls, Parkinson's Disease, Parkinson's Disease with MCI. HC: Healthy Controls; PD: Parkinson's Disease; PDM: PD with MCI. (B) The number of subjects where $z < 2$ in a specific electrode pair.

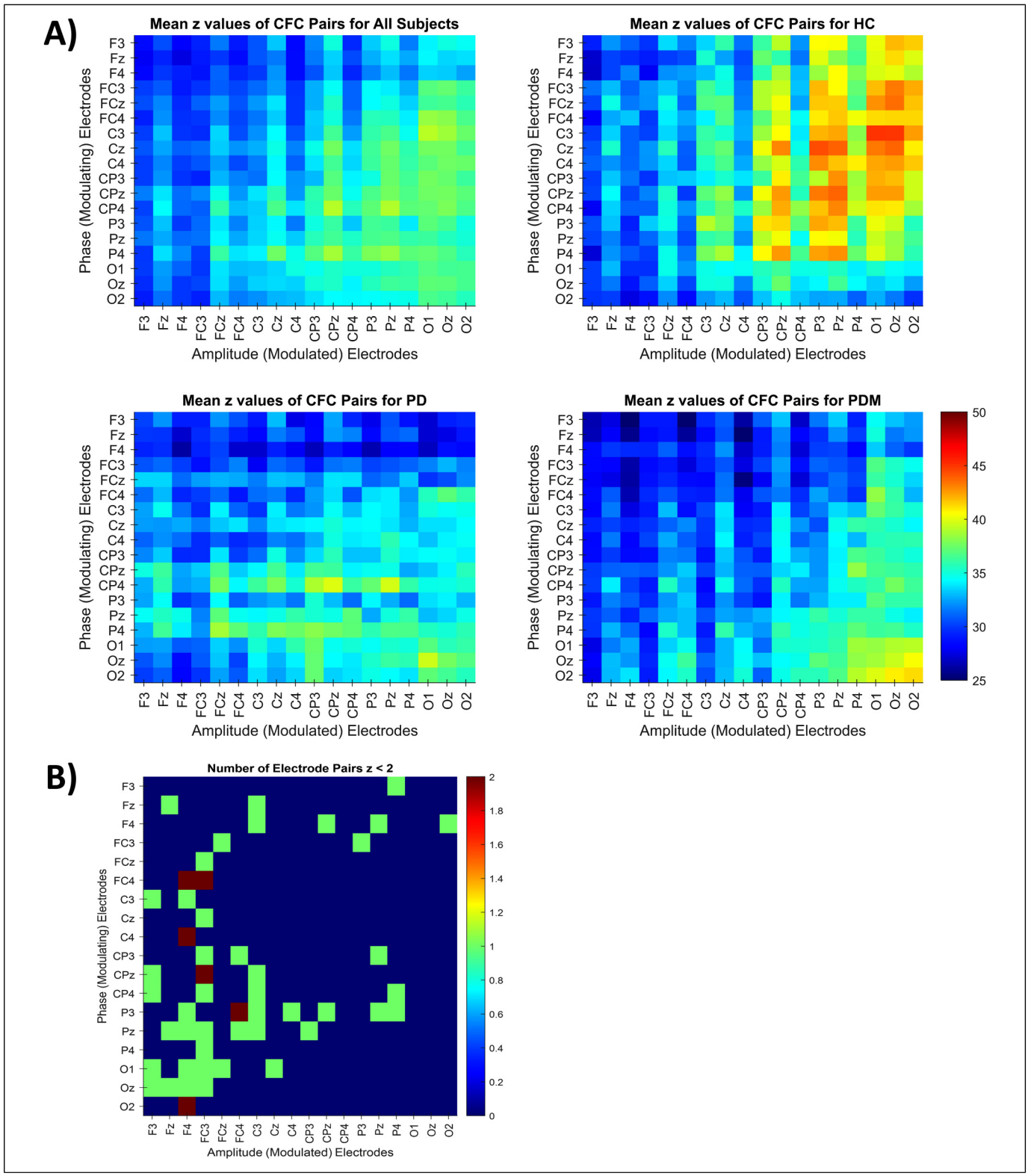

Figure 3. (A) Z values for delta-beta CFC between all electrode pairs. The mean z values for all subjects, healthy controls, Parkinson's Disease, Parkinson's Disease with MCI. HC: Healthy Controls; PD: Parkinson's Disease; PDM: PD with MCI. (B) The number of subjects where $z < 2$ in a specific electrode pair.

The most significant CFC based on PAC difference between the groups was found in anterior-to-posterior coupling. In the post-hoc tests, significant differences were consistently observed between the HC and PD groups as well as between the HC and PDMCI ($p < .05$). Therefore, the results of the anterior-to-posterior CFC value, which is the electrode pair where significant differences between the groups are observed, will be reported in the following paragraphs.

The direction of the CFC based on PAC at delta-theta was prominent from the anterior to the posterior scalp regions in all groups. In relation to the HC and PD groups, the PDMCI group was characterized by more posteriorly located CFC values (Supplementary Figure 1 and Figure 1; Tables 3a, 3b).

For the CFC based on PAC at delta-low frequency alpha, the prominent direction was anterior-to-posterior in the HC group. In contrast, that prominent direction was posterior-to-anterior in the PD and PDMCI groups, with an emphasis on right frontal electrode pairs (Supplementary Figure 2 and Figure 2; Tables 4a, 4b).

For the CFC based on PAC at delta-beta, the prominent direction was anterior-to-posterior in all groups. However, the CFC was lower especially at left electrode pairs in the PD and PDMCI groups as compared to the HC group (Supplementary Figure 3 and Figure 3; Tables 5a, 5b).

Table 3a. Delta – Theta CFC. Repeated Measures ANOVA Results Between Groups for the Within-Subject Factor of Location.

	Sum Sq.	DF	Mean Sq.	F	*pGG*
Intercept	10 521.0	3	3506.90	12.329	0.000
Group:Location	5901.5	6	983.58	3.458	***0.006***
Error	124 590	438	284.45		

*p*GG: Greenhouse-Gaisser corrected *p* values for non-sphericity.

Table 3b. Significant Group by Location Interactions for Delta-Theta CFC.

		Diff.	SE	*p*	Lower	Upper
AP	HC versus PD	13.154	4.138	*.004*	3.457	22.851
	HC versus PDM	12.279	4.034	*.007*	2.826	21.733
	PD versus PDM	−0.875	4.099	ns	−10.481	8.732

Lower and Upper limits of simultaneous 95% confidence intervals for the true differences.
Abbreviations: AP, anterior-to-posterior; HC, healthy controls; PD, Parkinson's disease; PDM, PD with MCI; Diff., difference; SE, standard error.

Table 4a. Delta – Low Frequency Alpha CFC. Repeated Measures ANOVA Results Between Groups for the Within-Subject Factor of Location.

	Sum Sq.	DF	Mean Sq.	F	*pGG*
Intercept	9007.5	3	3002.50	14.001	0.000
Group:Location	6543.4	6	1090.60	5.085	***0.000***
Error	93 286.0	435	214.45		

*p*GG: Greenhouse-Geisser corrected *p* values for non-sphericity.

Table 4b. Significant Group by Location Interactions for Delta-Low Frequency Alpha CFC.

		Diff.	SE	*p*	Lower	Upper
AP	HC versus PD	12.487	3.793	*.003*	3.598	21.376
	HC versus PDM	9.599	3.715	*.026*	0.892	18.306
	PD versus PDM	−2.888	3.775	ns	−11.734	5.959

Lower and Upper limits of simultaneous 95% confidence intervals for the true differences.
Abbreviations: AP, anterior-to-posterior; HC, healthy controls; PD, Parkinson's disease; PDM, PD with MCI; Diff., difference; SE, standard error.

Table 5a. Delta – Beta CFC. Repeated Measures ANOVA Results Between Groups for the Within-Subject Factor of Location.

	Sum Sq.	DF	Mean Sq.	F	*pGG*
Intercept	3467.3	3	1155.80	9.727	0.000
Group:Location	2332.7	6	388.78	3.272	***0.008***
Error	53 113	447	118.82		

*p*GG: Greenhouse-Geisser corrected *p* values for non-sphericity.

Table 5b. Significant Group by Location Interactions for Delta-Beta CFC.

		Diff.	SE	*p*	Lower	Upper
AP	HC versus PD	9.893	3.188	.005	2.422	17.364
	HC versus PDM	8.091	3.109	.025	0.803	15.378
	PD versus PDM	−1.802	3.158	ns	−9.205	5.600

Lower and Upper limits of simultaneous 95% confidence intervals for the true differences.
Abbreviations: AP, anterior-to-posterior; HC, healthy controls; PD, Parkinson's disease; PDM, PD with MCI; Diff., difference; SE, standard error.

Discussion

Here we tested the hypothesis that PDMCI patients may be characterized by abnormal CFC based on PAC from EROs recorded during counting visual target (rare) stimuli in an oddball task. A specific focus was on the CFC values at frontal and posterior electrode pairs in relation to typical impairment in frontal executive functions in PDMCI patients. The experimental design included HC and cognitively unimpaired PD patients as controls. Hilbert transform served to estimate instantaneous phase and amplitude of EROs from delta to gamma frequency bands, while modulation index computed CFC based on PAC from EROs at electrode pairs.

The main results showed significant CFC based on PAC at delta between the three groups. For the CFC based on PAC at delta-theta, the coupling direction was prominent from

anterior to posterior scalp regions in all groups. However, the PDMCI group showed that delta PAC was more posteriorly located compared to the HC and PD groups. For the CFC based on PAC at delta-low frequency alpha, the prominent coupling direction was anterior-to-posterior in the HC and posterior-to-anterior in the PD and PDMCI groups.

These findings complement previous results showing that EROs recorded during counting visual and auditory target (rare) stimuli in an oddball task presented main abnormalities at delta and theta frequency bands in PD patients with cognitive impairment when compared to HC persons.[10,11]

These results suggest that PDMCI patients may be characterized by reduced and more posterior topography of delta-theta, delta-low frequency alpha, and delta-beta CFCs as a reflection of the impairment of brain cognitive systems. According to Lakatos et al. (2005), there may be a hierarchy in the EROs at different frequency bands during the cognitive information processing of external stimuli. In PDMCI patients, abnormal CFCs at the low frequencies might reflect a derangement in the "initial processes" in this hierarchical neurophysiological mechanisms occurring during the processing of rare (target) stimuli in a visual oddball paradigm.[7] In this line, the reduced CFC at low-to-low alpha frequency prominent in the frontal areas found in the PDMCI patients may reflect an impairment in the long-range cortical functional connectivity within frontal-parietal attention systems underpinning frontal executive functions, which may be a precursor to low-to-beta CFC that have decreased in patients. "In all group" correlation results (see supplementary) also may indicate that the Stroop test scores, which measure frontal-executive functions, as well as the general cognitive scores, are deteriorating with the decrease of AP delta-beta CFC.

Another current finding in the PDMCI patients showed an altered direction in the CFC based on PAC at delta-low frequency alpha from EROs, especially the PDMCI patients. That direction reversed from the anterior-to-posterior in the HC persons to the posterior-to-anterior in the PDMCI patients. As the slow frequency oscillations are typically associated with functional inhibition mostly,[56–58] PDMCI patients may suffer from impaired inhibitory control from frontal to posterior cortical regions during cognitive information processing.[56–58]

In previous studies, frontal EROs at slow frequencies during cognitive tasks were supposed to be modulated by the dopaminergic system.[59,60] In that system, dopamine may cause neural inhibition or excitation according to its receptor.[61] Parker et al. (2014, 2015) showed the relationship between cortical EEG theta oscillations and the stimulation of D1 dopamine receptors which have inhibition effects.[60,62] Consistently, the present findings showed higher CFC based on PAC at delta-low frequency alpha from the anterior to the posterior direction in the HC group but not in the PD patient groups, especially PDMCI patients. Impaired directionality in the slow oscillatory CFC based on PAC in the PDMCI patients may depend on the impaired dopaminergic mechanisms during the cognitive processes of target stimuli probed by the visual oddball task. Future studies in PDMCI patients will have to correlate the present abnormalities in the CFC based on PAC and the dopaminergic disruption as revealed by neuroimaging techniques.

Conclusions

To our knowledge, the present study is the first study presenting the altered CFC based on PAC from EROs in PDMCI patients. As compared to the HC and PD groups, the PDMCI group was characterized by (1) more posterior topography of the CFC based on PAC at delta-theta, (2) reversed CFC based on PAC at delta-low frequency alpha, namely from anterior-to-posterior to posterior-to-anterior, and (3) reduced anterior-to-posterior CFC based on PAC at delta-beta. These results suggest that during cognitive demands, PDMCI patients are characterized by abnormal neurophysiological oscillatory mechanisms mainly led by delta frequencies underpinning functional connectivity from frontal to posterior cortical areas.

Declaration of Conflicting Interests

The author(s) declared no potential conflicts of interest with respect to the research, authorship, and/or publication of this article.

Ethical Approval

The study was approved by the local ethics committee of Istanbul Medipol University with decision no. 10840098-51.

Funding

The author(s) disclosed receipt of the following financial support for the research, authorship, and/or publication of this article: This work was supported by the The PDWAVES Consortium, The Scientific and Technological Research Council of Turkey (TÜBİTAK), (grant number grant number 214S111)

ORCID iDs

Duygu Hünerli Gündüz https://orcid.org/0000-0003-0278-258X
Bahar Güntekin https://orcid.org/0000-0002-0860-0524

Supplemental Material

Supplemental material for this article is available online.

References

1. Calabresi P, Picconi B, Tozzi A, Di Filippo M. Dopamine-mediated regulation of corticostriatal synaptic plasticity. *Trends Neurosci*. 2007;30(5):211-219. doi:10.1016/J.TINS.2007.03.001
2. Aarsland D, Brønnick K, Fladby T. Mild cognitive impairment in Parkinson's disease. *Curr Neurol Neurosci Rep*. 2011;11(4):371-378. doi:10.1007/s11910-011-0203-1
3. Aarsland D, Andersen K, Larsen JP, Lolk A, Nielsen H, Kragh-Sørensen P. Risk of dementia in Parkinson's disease. *Neurology*. 2001;56(6):730-736. doi:10.1212/WNL.56.6.730
4. Aarsland D, Andersen K, Larsen JP, Lolk A, Kragh-Sørensen P. Prevalence and characteristics of dementia in Parkinson disease:

an 8-year prospective study. *Arch Neurol*. 2003;60(3):387-392. doi:10.1001/ARCHNEUR.60.3.387
5. Hughes TA, Ross HF, Musa S, et al. A 10-year study of the incidence of and factors predicting dementia in Parkinson's disease. *Neurology*. 2000;54(8):1596-1603. doi:10.1212/WNL.54.8.1596
6. Babiloni C, Pascarelli MT, Lizio R, et al. Abnormal cortical neural synchronization mechanisms in quiet wakefulness are related to motor deficits, cognitive symptoms, and visual hallucinations in Parkinson's disease patients: an electroencephalographic study. *Neurobiol Aging*. 2020;91(JULY):88-111. doi:10.1016/j.neurobiolaging.2020.02.029
7. Lakatos P, Shah AS, Knuth KH, Ulbert I, Karmos G, Schroeder CE. An oscillatory hierarchy controlling neuronal excitability and stimulus processing in the auditory cortex. *J Neurophysiol*. 2005;94(3):1904-1911. doi:10.1152/jn.00263.2005
8. Jensen O, Colgin LL. Cross-frequency coupling between neuronal oscillations. *Trends Cogn Sci*. 2007;11(7):267-269. doi:10.1016/j.tics.2007.05.003
9. Yener GG, Fide E, Özbek Y, et al. The difference of mild cognitive impairment in Parkinson's disease from amnestic mild cognitive impairment: Deeper power decrement and no phase-locking in visual event-related responses. *Int J Psychophysiol*. 2019;139(MAY):48-58. doi:10.1016/j.ijpsycho.2019.03.002
10. Güntekin B, Hanoglu L, Güner D, et al. Cognitive impairment in Parkinson's disease is reflected with gradual decrease of EEG delta responses during auditory discrimination. *Front Psychol*. 2018;9(FEB):1-13. doi:10.3389/fpsyg.2018.00170
11. Güntekin B, Aktürk T, Yıldırım E, Yılmaz NH, Hanoğlu L, Yener G. Abnormalities in auditory and visual cognitive processes are differentiated with theta responses in patients with Parkinson's disease with and without dementia. *Int J Psychophysiol*. 2020;153(JULY):65-79. doi:10.1016/j.ijpsycho.2020.04.016
12. Emek-Savaş DD, Özmüş G, Güntekin B, et al. Decrease of delta oscillatory responses in cognitively normal Parkinson's disease. *Clin EEG Neurosci*. 2017;48(5):355-364. doi:10.1177/1550059416666718
13. Schmiedt C, Meistrowitz A, Schwendemann G, Herrmann M, Basar-Eroglu C. Theta and alpha oscillations reflect differences in memory strategy and visual discrimination performance in patients with Parkinson's disease. *Neurosci Lett*. 2005;388(3):138-143. doi:10.1016/j.neulet.2005.06.049
14. Schmiedt-Fehr C, Schwendemann G, Herrmann M, Basar-Eroglu C. Parkinson's disease and age-related alterations in brain oscillations during a simon task. *Neuroreport*. 2007;18(3):277-281. doi:10.1097/WNR.0b013e32801421e3
15. Güntekin B, Aktürk T, Arakaki X, et al. Are there consistent abnormalities in event-related EEG oscillations in patients with Alzheimer's disease compared to other diseases belonging to dementia? *Psychophysiology*. 2022;59(5):e13934. doi:10.1111/psyp.13934
16. Fries P. A mechanism for cognitive dynamics: Neuronal communication through neuronal coherence. *Trends Cogn Sci*. 2005;9(10):474-480. doi:10.1016/j.tics.2005.08.011
17. Demiralp T, Bayraktaroglu Z, Lenz D, et al. Gamma amplitudes are coupled to theta phase in human EEG during visual perception. *Int J Psychophysiol*. 2007;64(1):24-30. doi:10.1016/j.ijpsycho.2006.07.005
18. Bragin A, Jando G, Nddasdy Z, Hetke J, Wise K, Buzsirkil G. Gamma (40–100 Hz) oscillation in the hippocampus behaving rat. *J Neurosci*. 1995;15(1):47-60. https://www.jneurosci.org/content/15/1/47.short. Accessed April 22, 2021.
19. Muthuraman M, Bange M, Koirala N, et al. Cross-frequency coupling between gamma oscillations and deep brain stimulation frequency in Parkinson's disease. *Brain*. 2020;143(11):3393-3407. doi:10.1093/BRAIN/AWAA297
20. De Hemptinne C, Ryapolova-Webb ES, Air EL, et al. Exaggerated phase-amplitude coupling in the primary motor cortex in Parkinson disease. *Proc Natl Acad Sci U S A*. 2013;110(12):4780-4785. doi:10.1073/pnas.1214546110
21. Buzsáki G, Draguhn A. Neuronal olscillations in cortical networks. *Science (80-)*. 2004;304(5679):1926-1929. doi:10.1126/science.1099745
22. Weiss S, Mueller HM. "Too many betas do not spoil the broth": The role of beta brain oscillations in language processing. *Front Psychol*. 2012;3(JUN):1-15. doi:10.3389/fpsyg.2012.00201
23. Canolty RT, Knight RT. The functional role of cross-frequency coupling. *Trends Cogn Sci*. 2010;14(11):506-515. doi:10.1016/j.tics.2010.09.001
24. Lisman J, Idiart M. Storage of 7 ± 2 short-term memories in oscillatory subcycles. *Science (80-)*. 1995;267(5203):1512-1515. doi:10.1126/science.7878473
25. Axmacher N, Henseler MM, Jensen O, Weinreich I, Elger CE, Fell J. Cross-frequency coupling supports multi-item working memory in the human hippocampus. *Natl Acad Sci*. 2010;107(7):3228-3233. doi:10.1073/pnas.0911531107
26. Tort ABL, Komorowski RW, Manns JR, Kopell NJ, Eichenbaum H. Theta-gamma coupling increases during the learning of item-context associations. *Proc Natl Acad Sci U S A*. 2009;106(49):20942-20947. doi:10.1073/pnas.0911331106
27. Schroeder CE, Lakatos P. Low-frequency neuronal oscillations as instruments of sensory selection. *Trends Neurosci*. 2009;32(1):9-18. doi:10.1016/j.tins.2008.09.012
28. Cohen MX, Elger CE, Fell J. Oscillatory activity and phase-amplitude coupling in the human medial frontal cortex during decision making. *J Cogn Neurosci*. 2009;21(2):390-402. doi:10.1162/jocn.2008.21020
29. Händel B, Haarmeier T. Cross-frequency coupling of brain oscillations indicates the success in visual motion discrimination. *Neuroimage*. 2009;45(3):1040-1046. doi:10.1016/j.neuroimage.2008.12.013
30. Najjar R, Brooker RJ. Delta-beta coupling is associated with paternal caregiving behaviors during preschool. *Int J Psychophysiol*. 2017;112(FEB):31-39. doi:10.1016/j.ijpsycho.2016.11.014
31. Arnal LH, Doelling KB, Poeppel D. Delta-beta coupled oscillations underlie temporal prediction accuracy. *Cereb Cortex*. 2015;25(9):3077-3085. doi:10.1093/cercor/bhu103
32. Poppelaars ES, Harrewijn A, Westenberg PM, van der Molen MJW. Frontal delta-beta cross-frequency coupling in high and low social anxiety: an index of stress regulation? *Cogn Affect Behav Neurosci*. 2018;18(4):764-777. doi:10.3758/s13415-018-0603-7
33. Salimpour Y, Anderson WS. Cross-Frequency coupling based neuromodulation for treating neurological disorders. *Front Neurosci*. 2019;0(FEB):125. doi:10.3389/FNINS.2019.00125
34. Allen EA, Liu J, Kiehl KA, et al. Components of cross-frequency modulation in health and disease. *Front Syst Neurosci*. 2011;0(JULY 2011):59. doi:10.3389/FNSYS.2011.00059/BIBTEX
35. Zhang R, Ren Y, Liu C, et al. Temporal-spatial characteristics of phase-amplitude coupling in electrocorticogram for human temporal lobe epilepsy. *Clin Neurophysiol*. 2017;128(9):1707-1718. doi:10.1016/J.CLINPH.2017.05.020

36. Mazaheri A, Segaert K, Olichney J, et al. EEG Oscillations during word processing predict MCI conversion to Alzheimer's disease. *NeuroImage Clin*. 2018;17(September 2017):188-197. doi:10.1016/j.nicl.2017.10.009
37. Goodman MS, Kumar S, Zomorrodi R, et al. Theta-Gamma coupling and working memory in Alzheimer's dementia and mild cognitive impairment. *Front Aging Neurosci*. 2018;10(APR):1-10. doi:10.3389/fnagi.2018.00101
38. Babiloni C, Frisoni GB, Pievani M, et al. White matter vascular lesions are related to parietal-to-frontal coupling of EEG rhythms in mild cognitive impairment. *Hum Brain Mapp*. 2008;29(12):1355-1367. doi:10.1002/HBM.20467
39. Dauwan M, van Dellen E, van Boxtel L, et al. EEG-directed connectivity from posterior brain regions is decreased in dementia with Lewy bodies: A comparison with Alzheimer's disease and controls. *Neurobiol Aging*. 2016;41(MAY):122-129. doi:10.1016/J.NEUROBIOLAGING.2016.02.017
40. Teipel S, Grothe MJ, Zhou J, et al. Measuring cortical connectivity in Alzheimer's disease as a brain neural network pathology: Toward clinical applications. *J Int Neuropsychol Soc*. 2016;22(2):138-163. doi:10.1017/S1355617715000995
41. Muller AJ, Shine JM, Rolle CE, et al. Anterior-posterior electrophysiological activity characterizes parkinsonian visual misperceptions. *Neurol Clin Neurosci*. 2021;9(4):312-318. doi:10.1111/NCN3.12508
42. Hughes AJ, Daniel SE, Kilford L, Lees AJ. Accuracy of clinical diagnosis of idiopathic Parkinson's disease: A clinico-pathological study of 100 cases. *J Neurol Neurosurg Psychiatry*. 1992;55(3):181-184. doi:10.1136/jnnp.55.3.181
43. Litvan I, Goldman JG, Tröster AI, et al. Diagnostic criteria for mild cognitive impairment in Parkinson's disease: Movement disorder society task force guidelines. *Mov Disord*. 2012;27(3):349-356. doi:10.1002/mds.24893
44. Folstein MF, Folstein SE, McHugh PR. "Mini-mental state". A practical method for grading the cognitive state of patients for the clinician. *J Psychiatr Res*. 1975;12(3):189-198. doi:10.1016/0022-3956(75)90026-6
45. Güngen C, Ertan T, Eker E, Yaşar R, Engin F. [Reliability and validity of the standardized Mini mental state examination in the diagnosis of mild dementia in turkish population]. *Turk Psikiyatri Derg*. 2002;13(4):273-281. http://www.ncbi.nlm.nih.gov/pubmed/12794644. Accessed April 24, 2021.
46. Morris JC. The clinical dementia rating (cdr): Current version and scoring rules. *Neurology*. 1993;43(11):2412-2414. doi:10.1212/wnl.43.11.2412-a
47. Lang AET, Fahn S, Munsat TL. Assessment of Parkinson's disease. In: *Quantification of Neurologic Deficit*. Boston, MA: Butterworth; 1989:285-309.
48. Hoehn MM, Yahr MD. Parkinsonism: onset, progression, and mortality. *Neurology*. 2001;57(10):11-26.
49. Blankertz B, Tangermann M, Vidaurre C, et al. The Berlin brain-computer interface: Non-medical uses of BCI technology. *Front Neurosci*. 2010;4(DEC):1-17. doi:10.3389/fnins.2010.00198
50. Nolte G, Bai O, Wheaton L, Mari Z, Vorbach S, Hallett M. Identifying true brain interaction from EEG data using the imaginary part of coherency. *Clin Neurophysiol*. 2004;115(10):2292-2307. doi:10.1016/j.clinph.2004.04.029
51. Tort ABL, Komorowski R, Eichenbaum H, Kopell N. Measuring phase-amplitude coupling between neuronal oscillations of different frequencies. *J Neurophysiol*. 2010;104(2):1195-1210. doi:10.1152/jn.00106.2010
52. Bayraktaroglu Z, von Carlowitz-Ghori K, Losch F, Nolte G, Curio G, Nikulin VV. Optimal imaging of cortico-muscular coherence through a novel regression technique based on multi-channel EEG and un-rectified EMG. *Neuroimage*. 2011;57(3):1059-1067. doi:10.1016/j.neuroimage.2011.04.071
53. Hurtado JM, Rubchinsky LL, Sigvardt KA. Statistical method for detection of phase-locking episodes in neural oscillations. *J Neurophysiol*. 2004;91(4):1883-1898. doi:10.1152/jn.00853.2003
54. Hesterberg T, Monaghan S, Moore DS, Clipson A, Epstein R, Freeman WH. *Bootstrap Methods and Permutation Tests Companion Chapter 18 To the Practice of Business Statistics*. W. H. Freeman and Company; 2003.
55. Mauchly JW. Significance test for sphericity of a normal n-variate distribution. *Ann Math Stat*. 1940;11(2):204-209. doi:10.1214/aoms/1177731915
56. Chmielewski WX, Mückschel M, Dippel G, Beste C. Concurrent information affects response inhibition processes via the modulation of theta oscillations in cognitive control networks. *Brain Struct Funct*. 2016;221(8):3949-3961. doi:10.1007/s00429-015-1137-1
57. Dippel G, Mückschel M, Ziemssen T, Beste C. Demands on response inhibition processes determine modulations of theta band activity in superior frontal areas and correlations with pupillometry – implications for the norepinephrine system during inhibitory control. *Neuroimage*. 2017;157(AUGUST):575-585. doi:10.1016/j.neuroimage.2017.06.037
58. Mückschel M, Dippel G, Beste C. Distinguishing stimulus and response codes in theta oscillations in prefrontal areas during inhibitory control of automated responses. *Hum Brain Mapp*. 2017;38(11):5681-5690. doi:10.1002/hbm.23757
59. Parker KL, Chen K-H, Kingyon JR, Cavanagh JF, Narayanan NS. Medial frontal 4-Hz activity in humans and rodents is attenuated in PD patients and in rodents with cortical dopamine depletion. *J. Neurophysiol*. 2015;114(2):1310-1320. doi:10.1152/JN.00412.2015
60. Parker KL, Ruggiero RN, Narayanan NS. Infusion of D1 dopamine receptor agonist into medial frontal cortex disrupts neural correlates of interval timing. *Front Behav Neurosci*. 2015;0(NOVEMBER):294. doi:10.3389/FNBEH.2015.00294
61. Śmiałowski A, Bijak M. Excitatory and inhibitory action of dopamine on hippocampal neurons in vitro. Involvement of D2 and D1 receptors. *Neuroscience*. 1987;23(1):95-101. doi:10.1016/0306-4522(87)90274-0
62. Parker KL, Chen K-H, Kingyon JR, Cavanagh JF, Narayanan NS. D1-Dependent 4 Hz oscillations and ramping activity in rodent medial frontal cortex during interval timing. *J Neurosci*. 2014;34(50):16774-16783. doi:10.1523/JNEUROSCI.2772-14.2014